Asian Journal of Chemistry Vol. 18, No. 2 (2006), 891–899

Investigation of (Mo, W)C Based Cemented Carbides

M. MOIEN* and E. ALIZADEH
Department of Chemistry, University of Guilan, P.O. Box 1194, Rasht, Iran
E-mail: moien@guilan.ac.ir

This work reports a process for the production of an alloy powder (Mo, W) and a hard solid solution (Mo, WC). The process comprises reducing a mixture of molybdenum oxide or hydroxide and tungsten oxide or hydroxide to form an alloy powder and subjecting the alloy powder to carburization. Some typical characteristics of the (Mo, W)C based cemented carbide alloys have also been studied.

Key Words: (Mo, W)C, Cemented carbides.

INTRODUCTION

Tungsten carbide (WC) powder has been used as a main component with binder metals. However, increase of the demand for cemented carbides consisting mainly of WC requirements inevitably with a problem of natural resources and if WC can be replaced by other metal carbides, this substitution will have a great influence upon the industry.

Molybdenum monocarbide (MoC) is considered as a useful substitute, since this carbide has the same crystal structure, a simple hexagonal type, as WC. However, the existence of the hexagonal molybdenum monocarbide as a simple substance has remained in question and thus an attempt to stabilize molybdenum monocarbide has exclusively been carried out by forming a solid solution with tungsten carbide, which forms a continuous solid solution with hexagonal molybdenum monocarbide. This method was firstly reported by Dawihl[1], but this solid solution was not examined in detail and the commercial worth was not found in those days. Various investigations concerned with the formation of (Mo, WC) and (Mo, W)(C, N) have recently been made[2–6].

In this paper, a process for the production of (Mo, W)C using the fine mixed powders is discussed. The effects of replacement of tungsten by molybdenum in the form of continuous solid solution on the properties of cemented carbides are also examined.

EXPERIMENTAL

Fig. 1 shows the example of the flow diagram showing the production of the (Mo, W) mixed alloys. Mo and W powders were dissolved in 28% aqueous ammonia and the resulting ammonia salts were gradually neutralized with hydrochloric acid to precipitate. Then the mixed oxides were fired at 500°C in air and sintered. The mixed powder was charged in a nickel boat and subjected to reduction at 1000°C in a hydrogen stream to obtain an (Mo, W) powder. The

(Mo, W) powder was then mixed with carbon and ball milled for 36 h. The mixed powder was reacted at high temperature in various atmospheres to form complete (Mo, W)C. The (Mo, W)C was mixed with Ni and Co powders by wet process in an organic solvent, dried, compacted and sintered in vacuum at various temperatures. The samples were then lapped and microstructures of specimens were observed through optical microscope and scanning electron microscope. The microstructures of the carbide grains were investigated by transmission electron microscopy.

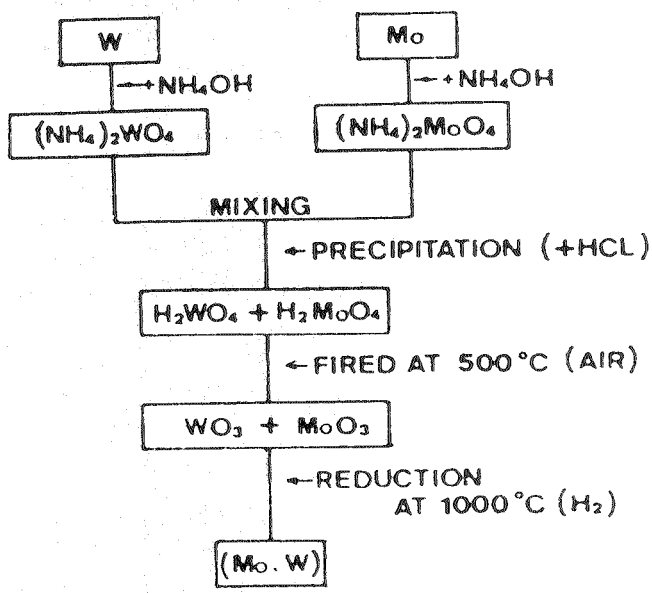

Fig. 1. Flow diagram showing the production of (Mo, W)

Various properties such as hardness, transverse rupture strength, oxidation resistance and coefficient of friction with steel were measured and compared with those of conventional WC based cemented carbides.

RESULTS AND DISCUSSION

Reaction Model

A reaction model was proposed to illustrate a process for producing (Mo, W)C which has a crystal structure of simple hexagonal. As is shown in Fig. 2, an (Mo, W)C mixed metal, which forms a continuous series of solid solutions, was prepared with a desired ratio of Mo to W. The alloy powder was converted into a complete (Mo, W)C powder by reacting it with carbon and heating it at a

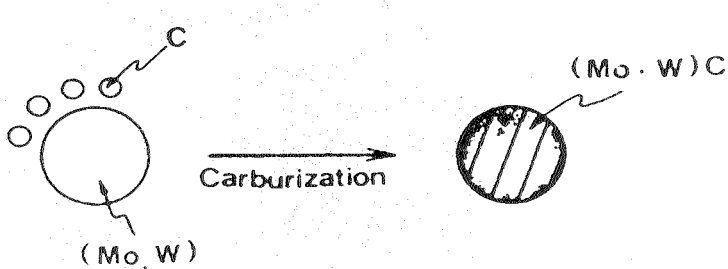

Fig. 2. Reaction model for producing (Mo, W)C

temperature of 1200°C or higher. If moylbdenum and tungsten are dispersed in atomic order, it is not necessary to use a diffusion aid such as iron. However, in order to increase the reduction speed, it is sufficient to add a trace amount of the diffusion aid during the production of mixed carbides.

(Mo, W) Mixed Alloys

Fig. 3 shows a scanning electron micrograph of the crystals of mixed oxides. The resulting mixed powder has such a small particle size that it can be converted into a solid solution at a relatively low temperature. It is also considered possible to obtain a solid solution by heating and diffusing the mixed metallic powder of W and Mo. However, in this method, reaction temperature to form complete solid solution is too high and pulverizing is troublesome.

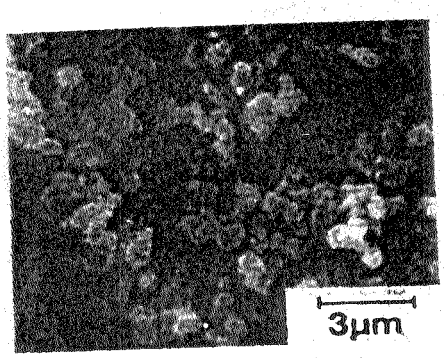

Fig. 3. Scanning electron micrograph of (Mo, W)O_3 powder

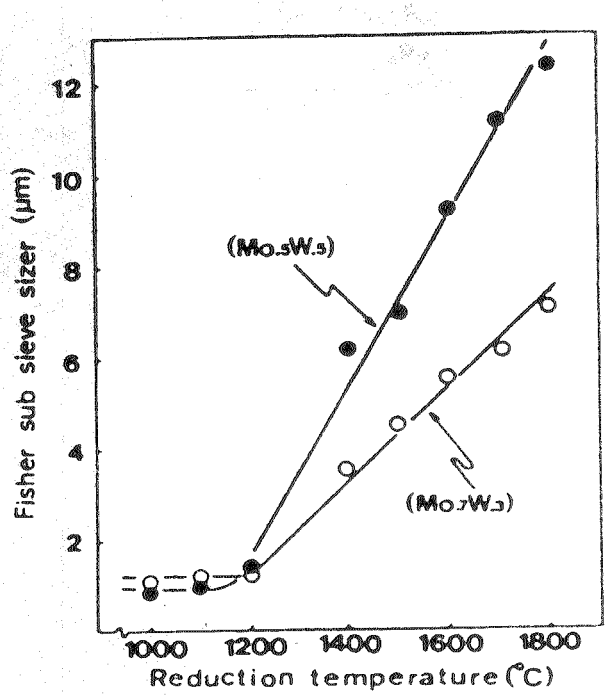

Fig. 4. Effect of reduction temperature on the grain growth of (Mo, W) powders

Fig. 4 shows the effect of reduction temperature on the grain growth of (Mo, W). Grain growth is dramatically accelerated above 1200°C. It is also found that more the exchange of Mo for W, lesser the grain growth of the grain. For example, when it is desired to obtain a coarse ($Mo_{0.7}W_{0.3}$) powder with the particle size of 6 μm, the reducing temperature should be at least 1600°C. Fig. 5 shows the micrographs of ($Mo_{0.7}W_{0.3}$) alloy powders. As the temperature increases, grains bond each other to form chain shaped particles.

The effect of the addition of sodium and potassium on the grain growth of (Mo, W) mixed metals was also examined. A particle promoter such as sodium and potassium is added at the amount of 2000 ppm before the reduction of mixed oxides with hydrogen. As is shown in Fig. 6–8, the particle growth is promoted by adding dopants such as sodium and potassium.

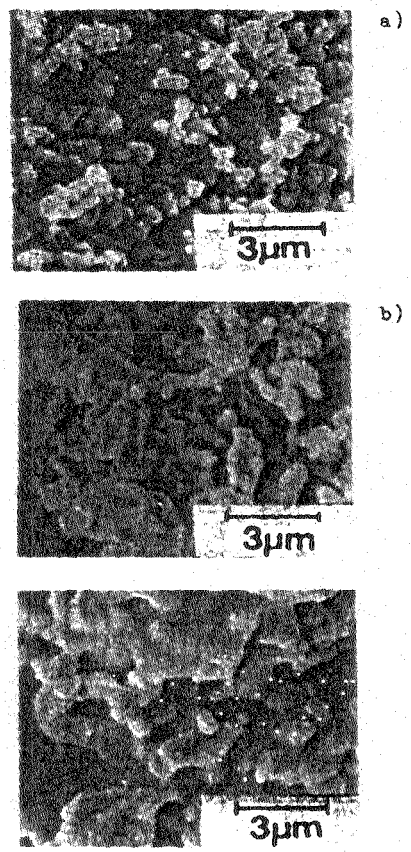

Fig. 5. Scanning electron micrographs of $(Mo_{0.7}W_{0.3})$ at various reduction temperatrues
(a) 1200°C for 30 min.
(b) 1400°C for 30 min.
(c) 1600°C for 30 min.

Fig. 6. Scanning electron micrograph of $(Mo_{0.7}W_{0.3})$ [No additive]

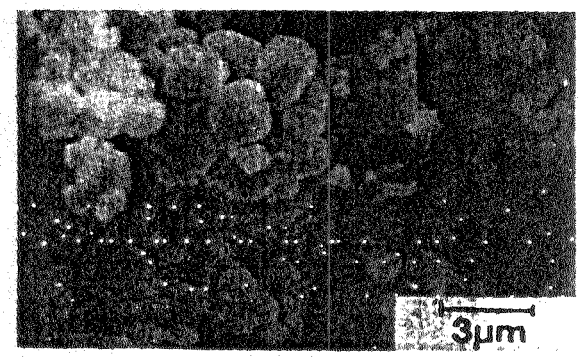

Fig. 7. Scanning electron micrograph of $(Mo_{0.7}W_{0.3})$ [Na: 2000 ppm]

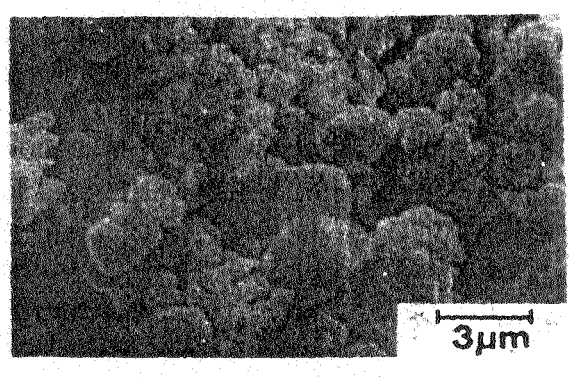

Fig. 8. Scanning electron micrograph of $(Mo_{0.7}W_{0.3})$ [K: 2000 ppm]

(Mo, W)C Mixed Carbides

The alloy powder obtained was then carburized by reacting with carbon. Fig. 9 shows the effect of carburizing temperature on the reactivity of (Mo, W)C. The reactivity of carbides means the ratio of combined carbon to theoretical carbon of the mixd carbides. In these carburizing conditions, it is found that

$(Mo_{0.5}W_{0.5})C$ is easier to carburize than $(Mo_{0.7}W_{0.3})C$. This is mainly because the diffusivity of C in Mo is much less than that of C in W. This is also one of the main reasons for the low reactivity at high temperatures, as in the case of the carburization of $(Mo_{0.7}W_{0.3})C$ with relatively coarse grains, is that the mixed carbide partly decomposes[2] into C and (Mo, W_3C_2) at around 1700°C.

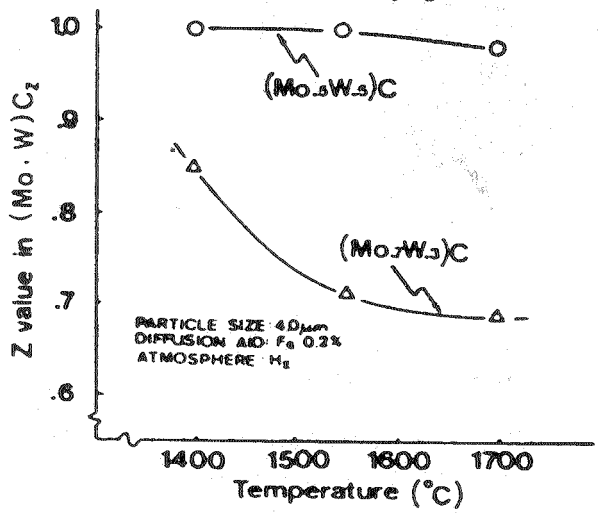

Fig. 9. Effect of carburizing temperature on the reactivity of (Mo, W)C

In order to increase the reactivity of $(Mo_{0.7}W_{0.3})C$ various carburizing conditions were examined. Table-1 demonstrates the suitability of the carburizing conditions for the production of $(Mo_{0.7}W_{0.3})C$. In order to get $(Mo_{0.7}W_{0.3})C$ with full reactivity, one method is to carburize in a nitrogen atmosphere and another method is to carburize at relatively high temperature followed by cooling to room temperature and reheating it up to 1400°C in a hydrogen atmosphere.

TABLE-1
SUTIABILITY OF CARBURIZING CONDITIONS
FOR THE PRODUCTION OF $(Mo_{0.7}W_{0.3})C$

Atmosphere	Temperature (°C)	Time (h)	T.C.	F.C.	C.C.	Reactivity (%)
N_2	1400	1	8.97	0.05	8.92	100
(1) H_2	1700	1	8.92	0.02	8.90	100
(2) H_2	1400	1				

Particle size: 4.0 μm
Diffusion aid: Iron 0.2%

The micrograph of $(Mo_{0.7}W_{0.3})C$ is shown in Fig. 10. The shape of $(Mo_{0.7}W_{0.3})C$ is characterized with triangular particles. It was also found that more the exchange of Mo for W of the mixed carbide, more the probability of triangular particles.

Fig. 11 demonstrates the effect of carburizing temperatures on the grain growth of (Mo, W)C. The grain growth of (Mo, W)C is much less than that of the (Mo, W) mixed alloys. Therefore, it is more advantageous to get coarse carbides by carburizing coarse mixed alloys and carbon at relatively low temperatures.

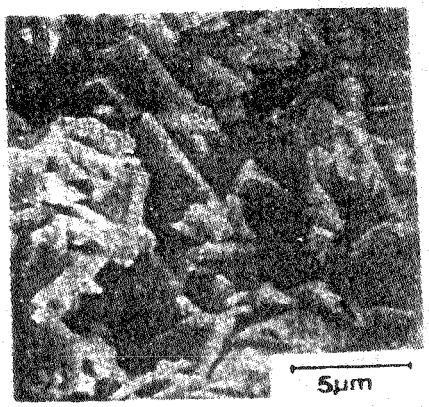

Fig. 10. Scanning electron micrograph of $(Mo_{0.7}W_{0.3})C$

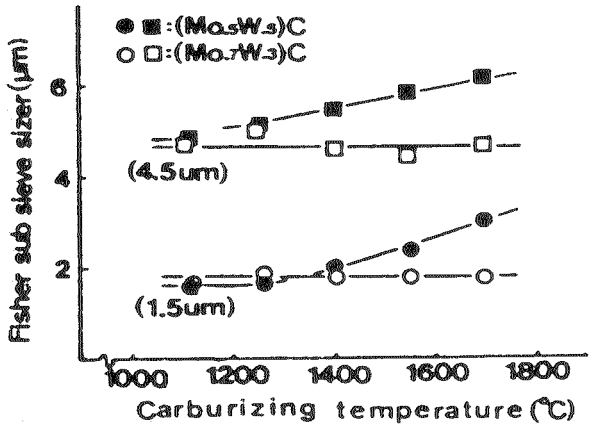

Fig. 11. Effect of carburizing temperature on the grain growth of (Mo, W)C

(Mo, WC) Based Cemented Carbides

(a) Microstructure: The transmission electron micrograph of a WC-Co alloy is shown in Fig. 12. Dislocation networks in the WC phase are observed in the WC grain. Fig. 13 shows the transmission electron micrograph of a $(Mo_{0.7}W_{0.3})C$-Co alloy. By making an electron diffraction of the parts using the selected area method, it was found that the orientation of the foil was (001) and that all of the interference fringes were on (100). In addition, as is seen in Fig. 13, $(Mo_{0.7}W_{0.3})C$ is heavily deformed with a high dislocation density. Fig. 14 shows another view of the $(Mo_{0.7}W_{0.3})C$-Co alloy by transmission electron microscopy.

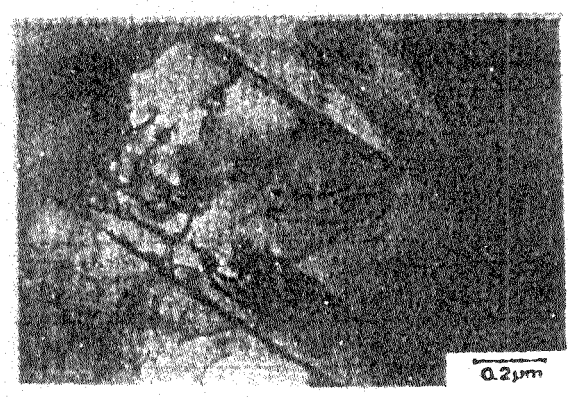

Fig. 12. Microstructure of WC grain by transmission electron microscopy

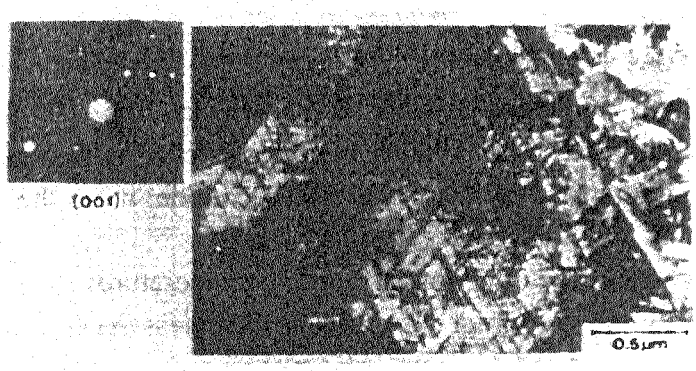

Fig. 13. Microstructure of $(Mo_{0.7}W_{0.3})C$ by transmission electron microscopy (001)

Fig. 14. Microstructure of $(Mo_{0.7}W_{0.3})C$ by transmission electron microscopy (311)

The orientation of the foil is (311). The parallel slip planes exist in the carbide grain. From these figures, it is confirmed that (Mo, W)C grains are more deformable than WC grains.

Fig. 15 and Fig. 16 show the microstructures of $(Mo_{0.5}W_{0.5})C$ 10% Ni-10% Co alloy and $(Mo_{0.7}W_{0.3})C$ 10% Ni-10% Co alloy respectively. The dark portion is the carbide phase and the white portion represents the binder metal phase. The mean particle size of the carbides of the alloy is about 4 μm.

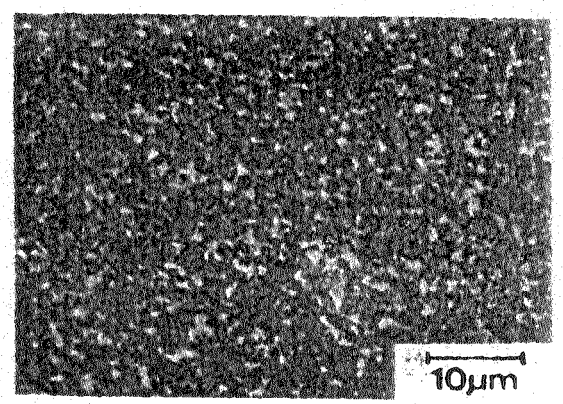

Fig. 15. Microstructure of $(Mo_{0.5}W_{0.5})C$-10% Co-10% Ni alloy

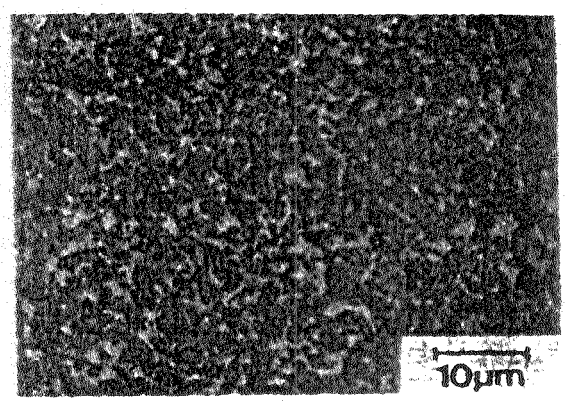

Fig. 16. Microstructure of $(Mo_{0.7}W_{0.3})C$ 10% Co-10% Ni alloy

(b) Properties: Fig. 17 shows the hardness of alloys with the binder phase of 10% Co-10% Ni. In the case of $(Mo_{0.7}W_{0.3})C$ base and $(Mo_{0.9}W_{0.1})C$ base hard alloys, the lower the carbon content, the lower the hardness. This is because M_2C_2 phase precipitates into the matrix and this phase lowers the hardness. However, in the case of $(Mo_{0.5}W_{0.5})C$ base cemented carbides, at lower carbon contents brittle M_6C phase precipitates into the matrix instead of M_2C phase and this phase increases the hardness of this alloy.

Fig. 18 demonstrates the effect of the carbon content on transverse rupture strength of alloys. One of the characteristics of this figure is that the higher the ratio of Mo to W in the carbide phase, the lower the carbon content of the maximum of transverse rupture strength. The reason why transverse rupture strength of $(Mo_{0.5}W_{0.5})C$ base alloys drastically decreases is because of the

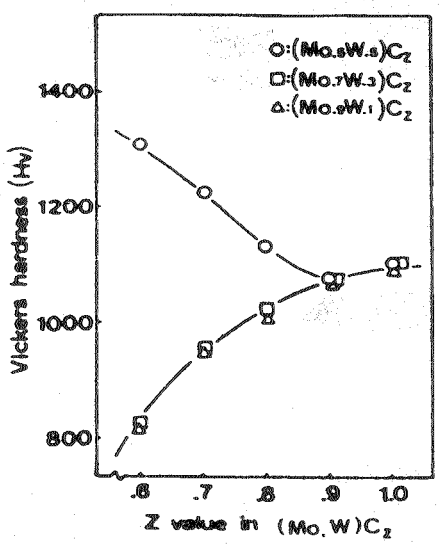

Fig. 17. Hardness of (Mo, W)C-Co-10%Ni alloys

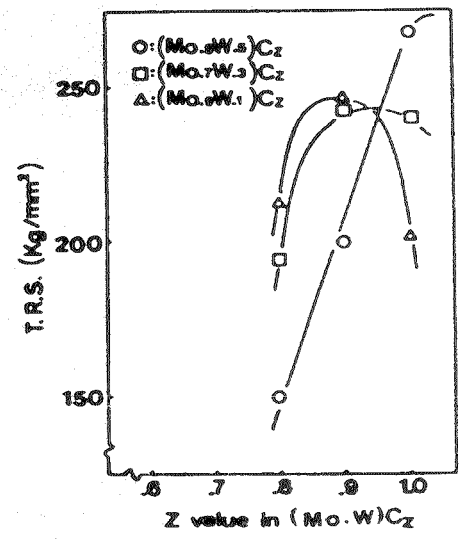

Fig. 18. Transverse rupture strength of (Mo, W)C-Co-10% Ni alloys

formation of M_6C at low carbon content. However, in the range of 0.97 to 1.00, which is MC + y region, $(Mo_{0.5}W_{0.5})C$ base alloy has the highest value of transverse rupture strength.

(Mo, W)C base cemented carbides have some remarkable characteristics with the addition of Mo in the hard phase. Fig. 19 presents the relations between the weight gain and the oxidation temperature. The tests were conducted in flowing air with a pressure of 1 atm. and the time the alloys were in the furnace at 1000°C was for 5 h. The weight gain of the WC base alloy was dramatically increased above 700°C. In contrast, that of the $(Mo_{0.7}W_{0.3})C$ base alloy did not change very much. Thus it can be noted that the (Mo, W)C base alloy is superior to the WC base alloy concerning oxidation resistance.

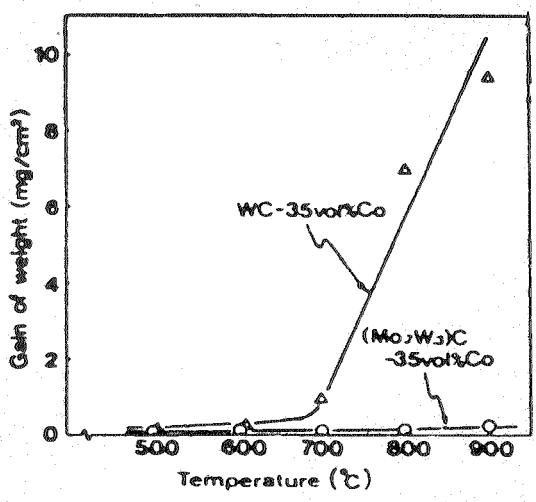

Fig. 19. Relations between gain of weight and temperature under the condition in air for 5 h

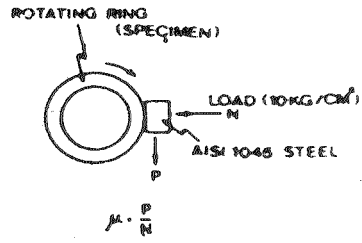

Fig. 20. Schematic diagram of apparatus measuring coefficient of friction

Another characteristic of (Mo, W)C base alloys is chemical reaction with steel. Fig. 20 shows a schematic diagram of the apparatus measuring coefficient of

friction between the specimen and steel. Load was vertically applied to the specimen with a magnitude of 10 kg/cm^2. The ring specimen was rotated at certain speeds and horizontal forces were measured by a dynamometer. Fig. 21 shows the results of the test. Coefficient of friction of the (Mo, W)C alloy is almost half that of the WC base hard alloy. It turns out that the (Mo, W)C base alloy has less chemical reaction with steel than conventional WC base alloy.

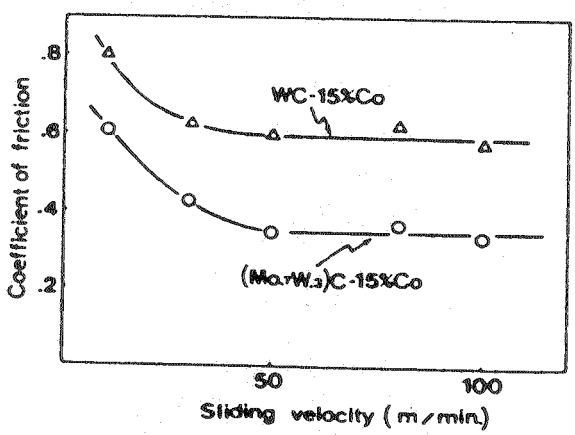

Fig. 21. Effect of sliding velocity on coefficient of friction

Conclusions

- By using (Mo, W) mixed metals as a starting material, the uniform monocarbide (Mo, W)C can be obtained at relatively low temperature.
- Regarding the production of coarse (Mo, W)C, elevation of reduction temperature is more effective than of carburizing temperature.
- It may be noted that (Mo, W)C grains are more deformable than WC grains.
- It is confirmed that (Mo, W)C base cemented carbides have better oxidation resistance and less chemical reaction with steel than conventional WC base cemented carbides.

ACKNOWLEDGEMENT

The authors wish to thank Mr. T. Nishikawa for operation of transmission electron microscope and performing the X-ray analyses.

REFERENCES

1. W. Dawihk, German Patent No. 900615 (1984).
2. E. Rudy, B.F. Kieffer and E. Baroch, *Planseeberichte fur Pulvermetallurgy*, **26**, 105 (1983–1988).
3. R. Kieffer, P. Ettmayer and B. Lux, Paper presented at Recent Advances in Hardmetal Production, Loughborough University, p. 33 (1990).
4. S. Yie, United States Patent No. 4049380 (1989).
5. P. Ettmayer, United States Patent No. 4212671 (1989).
6. M. Miyake, United States Patent No. 4216009 (1989).

(*Received*: 31 January 2005; *Accepted*: 15 November 2005) AJC-4505